



# Mapping of subsurface geological structures and depth to the top of magnetic basement in Bornu Basin and its environs, NE Nigeria, for possible hydrocarbon presence

Taiwo Adewumi<sup>1,2,3</sup> · Adeyinka Kazeem Salako<sup>2</sup> · Nordiana Mohd Muztaza<sup>3</sup> · Usman Defyan Alhassan<sup>2</sup> · Emeka Emmanuel Udensi<sup>2</sup>

Received: 1 March 2022 / Accepted: 3 September 2022

© Saudi Society for Geosciences 2022

## Abstract

The present study aims to provide a new insight into the subsurface geological structures and the depth estimates of the sediments aiding hydrocarbon maturation and accumulation within the Bornu Basin, NE Nigeria, via 2D magnetic structural and depth modelling. The total magnetic field anomaly map was reduced to the magnetic equator (RTE-TMI) to align the magnetic anomalies over their causative bodies. The resulting RTE-TMI map and the first- and second-order vertical derivative maps distinctively mapped the intra-sedimentary volcanic rocks and shallow to deep-seated structures. On the other hand, the source parameter imaging (SPI) and 2D depth constrained magnetic anomaly models determined the depths of these geologic features. The dominant structures within the study area trend NE-SW, NNE-SSW, ENE-WSW, ESE-WNW and NW-SE. SPI model indicated that the thickness of sedimentary beds ranges from 1.02 to 5.55 km, with a maximum thickness of  $\geq 3.0$  km obtained in the central, central eastern, southwestern, northeastern, eastern and western parts of the study area, corresponding to Gubio, Gadayi, Nafada, Marte, Dikwa and Gabdam, respectively. The 2D magnetic depth models from the seven profiles taken on the RTE-TMI map in N-S and SE-NW across significant anomalies revealed lithological boundaries and the thickness of sediments ranging from 1.0 km to a maximum thickness of 11.5 km. The thickness of sediments of 3.0 to 11.5 km is sufficient for hydrocarbon maturation and accumulation in Bornu Basin (a typical rift basin), with the delineated embedded structures serving as migratory paths or traps for the generated hydrocarbons.

**Keywords** 2D magnetic depth modelling · Bornu Basin · Hydrocarbon accumulation · Magnetic anomaly derivatives · Source parameter imaging (SPI) · Sedimentary basin

---

Responsible Editor: Santanu Banerjee

✉ Taiwo Adewumi  
taiwo.adewumi@science.fulafia.edu.ng;  
tydon4real@yahoo.co.uk

Adeyinka Kazeem Salako  
s.kazeem@futminna.edu.ng

Nordiana Mohd Muztaza  
mmnordiana@usm.my

<sup>1</sup> Department of Physics, Faculty of Science, Federal University of Lafia, Lafia, Nigeria

<sup>2</sup> Department of Geophysics, School of Physical Science, Federal University of Technology, Minna, Nigeria

<sup>3</sup> School of Physics, Universiti Sains Malaysia (USM), Penang 11800, Malaysia

## Introduction

Airborne magnetic data has been extensively and effectively used in the mapping of subsurface geological structures for mineral exploration (Adewumi and Salako 2018; Ekwok et al. 2020; Eldosouky et al. 2021; Elkhateeb et al. 2021), potential paths for hydrocarbon migration (Selim and Aboud 2012; Anudu et al. 2014), basement architecture and topography (Razavi Pash et al. 2021; Nabilou et al. 2022; Saada et al. 2022), heat flow for geothermal sources (Melouah et al. 2021; Adewumi et al. 2021; Awoyemi et al. 2022) and thickness of sediments for hydrocarbon prospecting (Salako and Udensi 2015; Adewumi et al. 2017; Arogundade et al. 2020). Delineation of the edges and geologic deep-to-shallow structures from potential field sources such as magnetic data provides a fundamental tool for interpreting geological structures (Eldosouky et al.

2022). The characterisation of magnetic anomalies in oil and gas deposits reveals various lithological and structural factors imperative in hydrocarbon exploration. Subsurface geological structures (faults, lineaments, salt diapirs, etc.) and sediment thickness estimation are critical in hydrocarbon exploration because they control oil and gas migration and hydrocarbon maturation within sedimentary basins, respectively. The search for hydrocarbon prospectivity in an area using magnetic methods is aimed at delineating favourable geological structures and the thickness of sediments that might support the generation, accumulation and migration of hydrocarbons in a sedimentary basin (Talwani and Walter 2003).

The Bornu Basin, the study area, is one of the sedimentary basins in Nigeria thought to have hydrocarbon potential due to some favourable geological factors that correlate with the contiguous Termit Basin, and the mega Chad Basin in the Niger and Chad Republics, where hydrocarbons (oil and gas) have been discovered and exploited in commercial quantities (Genik 1993). To increase Nigeria's hydrocarbon reserves, the Nigerian government has drilled at least 23 dry exploratory wells in the Bornu Basin (a sub-basin of the Chad Basin), which have yielded little or no result in terms of commercial exploration of oil and gas. The source rock evaluation carried out along the wells (Wadi and Kinasar) in the Fika shale and Gongila formation at the depths of 1290 m, 1670 m, 2180 m, 2280 m and 2935 m comprised of siltstones and mudstone characterized with variable organic matter shows the low content of organic matter in some of the wells. These features reduced hydrocarbon exploitation in commercial quantity (Ola 2018; Ogungbesan et al. 2020), hence the need to further investigate the basin using geophysical methods to map the subsurface crustal architecture to ascertain the hydrocarbon potentiality in the study area.

The search for hydrocarbons in the Bornu Basin began several years ago with the use of magnetic and gravity data, employing enhancement techniques such as spectral depth imaging, source parameter imaging, wavelet analysis and Euler deconvolution, to determine the depth to the top of the geologic sources, sediment thickness and geologic structures for possible hydrocarbon maturation and accumulation (Isogun 2005; Anakwuba et al. 2011; Anakwuba and Augustine 2012; Ajana et al. 2014; Salako 2014; Lawal et al. 2015; Salako and Udensi 2015; Aderoju et al. 2016; Akiishi et al. 2019; Arogundade et al. 2020; Akanji et al. 2020; Awoyemi et al. 2022; Ekwok et al. 2022). Therefore, this study attempts to delineate subsurface litho-structural architecture controlling hydrocarbon maturation and accumulation within the Bornu Basin using 2D structural and magnetic depth modelling via a rose diagram and vertical derivatives of aeromagnetic data compared to previous studies.

## Location and geologic settings of the study area

The study area is located in northeastern Nigeria, within the southwestern part of the Chad Basin, locally known as the Bornu Basin, and its environs, bounded by longitudes 11.00°E to 14.00°E and latitudes 11.00°N to 13.00°N (Fig. 1). The basin falls within the Cretaceous sedimentary terrain (Fig. 1). It occupies one-tenth of the Chad Basin and is bordered to the north, northeast and east by the Republic of Niger, Chad and Cameroon. The Bornu Basin is separated from the other interior basins in Nigeria by the Zumbuk ridge (Okpikoro and Olorunniwo 2010) and the Dumbulwa-Bage High (Obaje et al. 2004; Zaborski et al. 1998). To the south, the Benue Trough is marked by strong magmatism linked with the Gulf of Guinea's entry (Guiraud et al. 1992; Emujakporue et al. 2012) and has a geometry similar to the Cameroon Volcanic Line (Guiraud et al. 1992; Emujakporue et al. 2012). The Bornu Basin and its adjoining Benue Trough have significant stratum sequence differences (Obaje et al. 2004; Abubakar 2014; Isyaku et al. 2016).

Various studies have described the geology of the Bornu Basin as vast sediment-filled subsidence in the northeastern section of Nigeria and bordering areas of the Republic of Chad (Okosun 1992, 1995; Olugbemiro et al. 1997; Obaje 2009; Olabode et al. 2015). In the southern region of the West African Rift System, the Bornu Basin is an intracratonic rift basin. It is one of the basins in the West Central African Rift System (WCARS), which includes the West African Rift Subsystem (WARS) in Algeria, Niger, Nigeria and Chad, as well as the Central African Rift Subsystem (CARS) in Chad, Cameroon and the Central African Republic (Genik 1992; Okosun 1995; Ahmed et al. 2022). Rift basins worldwide are quite important for hydrocarbon exploration (e.g., Dasgupta and Mukherjee 2017 2019; Dasgupta et al. 2022; Kar et al. 2022; Biswas et al. *in press*). The lower Cretaceous to Neogene sediments with a thickness of 3–12 km settled in the fluvial, lacustrine and marine environment of the Bornu Basin (a Cretaceous-Tertiary rift basin) (Genik 1992, 1993; Zanguina et al. 1998). In the Bornu Basin's Cretaceous-Tertiary rifts, the average depth to the top of the basement for oil windows is between 2500 and 4000 m.

The study area comprises different formations (lithological units) (Figs. 2 and 3). The Chad Formation (CF) is the predominant and youngest formation with a Quaternary sediment sequence of fine to coarse-grained sand clay, occupying the northern and eastern parts of the study area. It overlies formations such as the Keri-Keri Formation (KF) in the southern and southwestern parts, which overlies the Yolde Formation (YF) in the southern part. The Pindiga Formation (PF) in the southwestern

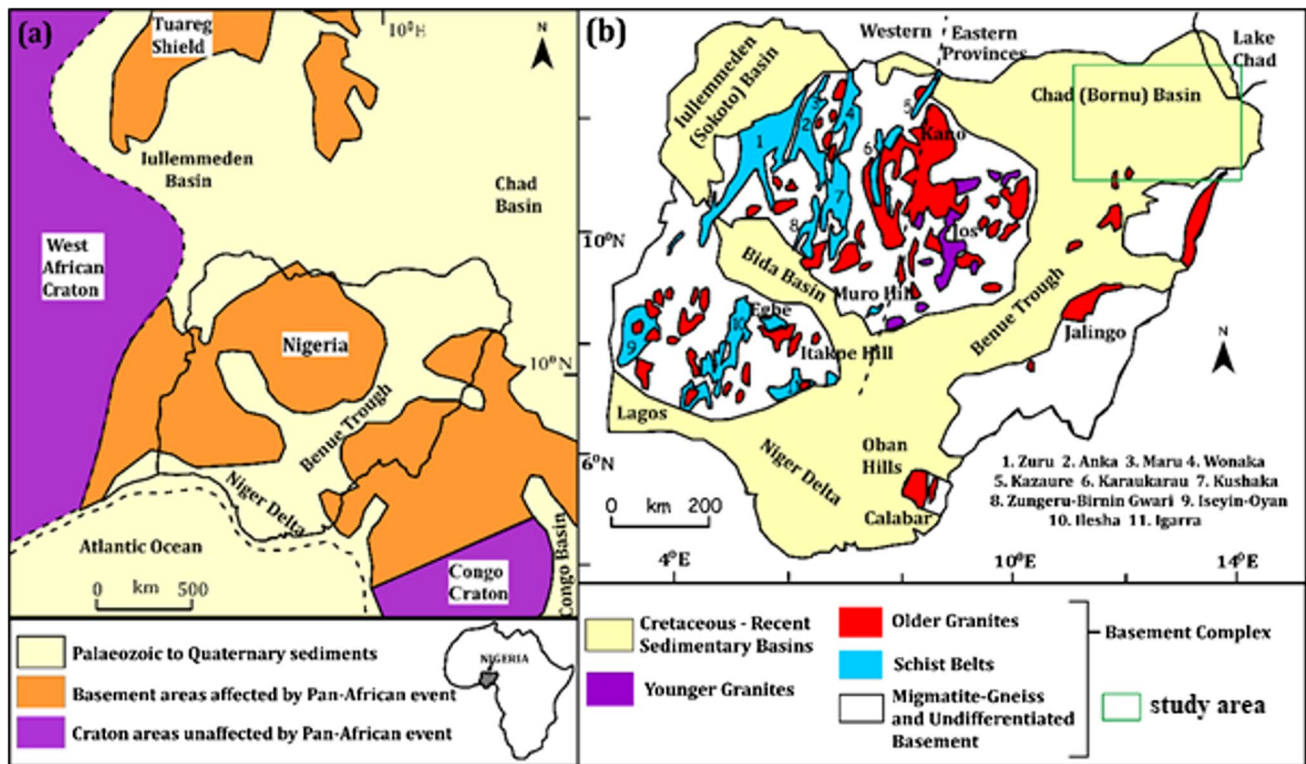


**Fig. 1** a Nigeria’s regional geological map and b the detailed regional geological map of Nigeria showing the Southwestern Basement Complex (modified after Woakes et al. 1987)

part conformably overlies the YF and the Bima Formation (BF). In contrast, the Gombe Formation (GF) in the southwestern part unconformably lies on the PF. The YF and BF unconformably underly the PF in the southern part of the study area (Fig. 2).

**Methodology**

**Airborne magnetic data**

The airborne magnetic dataset used in this study was acquired from the Nigerian Geological Survey Agency (NGSA). The airborne geophysical surveys were conducted between the years 2005 and 2009 by Fugro Airborne Survey on behalf of NGSA (NGSA 2005). The magnetic datasets were collected using a 3X Scintrex CS3 Cesium Vapour Magnetometer using acquisition parameters including an acquisition. Data were collected at an interval of 0.1 s at an altitude of 100 m along a flight line spacing of 500 m in NW–SE, a sensor mean terrain clearance of 80 m, a tie line spacing of 2 km and a flight line trend of 125°. For a half-degree sheet, the maps were created on a scale of 1:100,000. Using the International Geomagnetic Reference Field (IGRF) of 2005, the geomagnetic gradient was

eliminated from the aeromagnetic data. The following steps were employed to achieve the aim and objectives of this study.

- (i) Assembling and knitting of the twenty-four aeromagnetic data sheets covering the study area to produce the total magnetic intensity (TMI) map using Oasis Montaj software.
- (ii) Reduction of the TMI map to the magnetic equator (RTE) to position of the anomalies observed in the area over their causative bodies.
- (iii) Delineating the geological structures serving as migratory paths/traps for hydrocarbon accumulation within the study area using vertical derivatives and rose diagram and also map the basement architecture and topography from 2D aeromagnetic modelling
- (iv) Mapping the depth to top of the magnetic basement for depth constraint for the modelling using source parameter imaging.

**Geological structural mapping**

**Vertical derivative**

In regions with a lack of rock exposures and poor accessibility, such as the study area (Bornu Basin), different orders

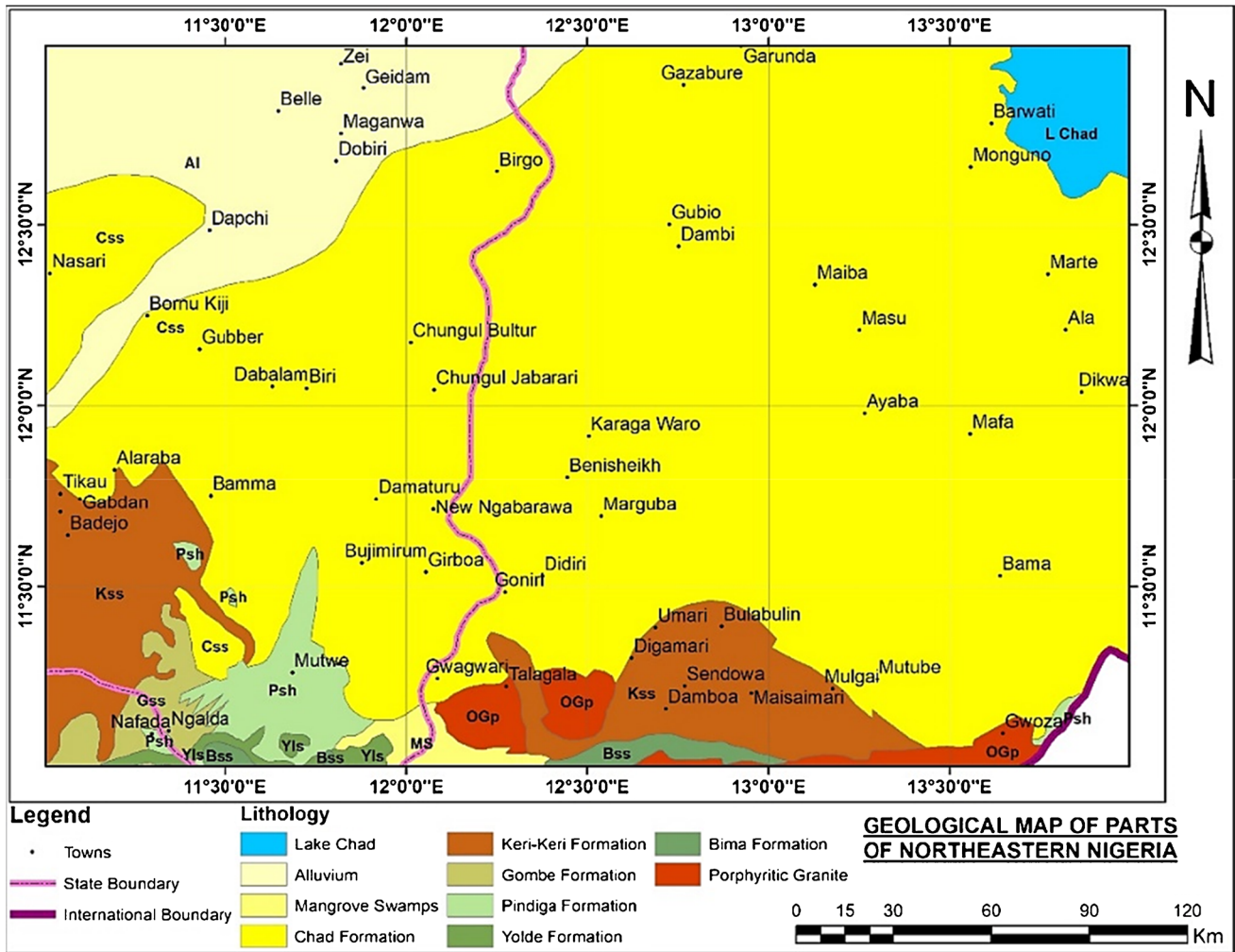


Fig. 2 Study area’s geological map (digitized from the regional geological map of Nigeria)

(first and second orders) of vertical derivative (VD) filtering are effective tools for mapping intra-sedimentary volcanic rocks and geological structures (Anudu et al. 2014). Vertical derivatives generally highlight the borders of anomalies and improve the physical representation of shallow causative geological formations. VD also narrows anomaly widths and precisely recognises or detects geological body contacts/boundaries (Cooper and Cowan 2004). Hence, it is used in this study to delineate geological structures that might serve as migratory paths/traps for hydrocarbon accumulation within the study area. The first- and second-order vertical derivatives are defined as follows (Anudu et al. 2014):

$$FVD = -\left(\frac{\partial T}{\partial z}\right) \tag{1}$$

$$SVD = \left(\frac{\partial^2 T}{\partial z^2}\right) \tag{2}$$

where FVD is the first vertical derivative, SVD is the second vertical derivative and *T* is the total magnetic field.

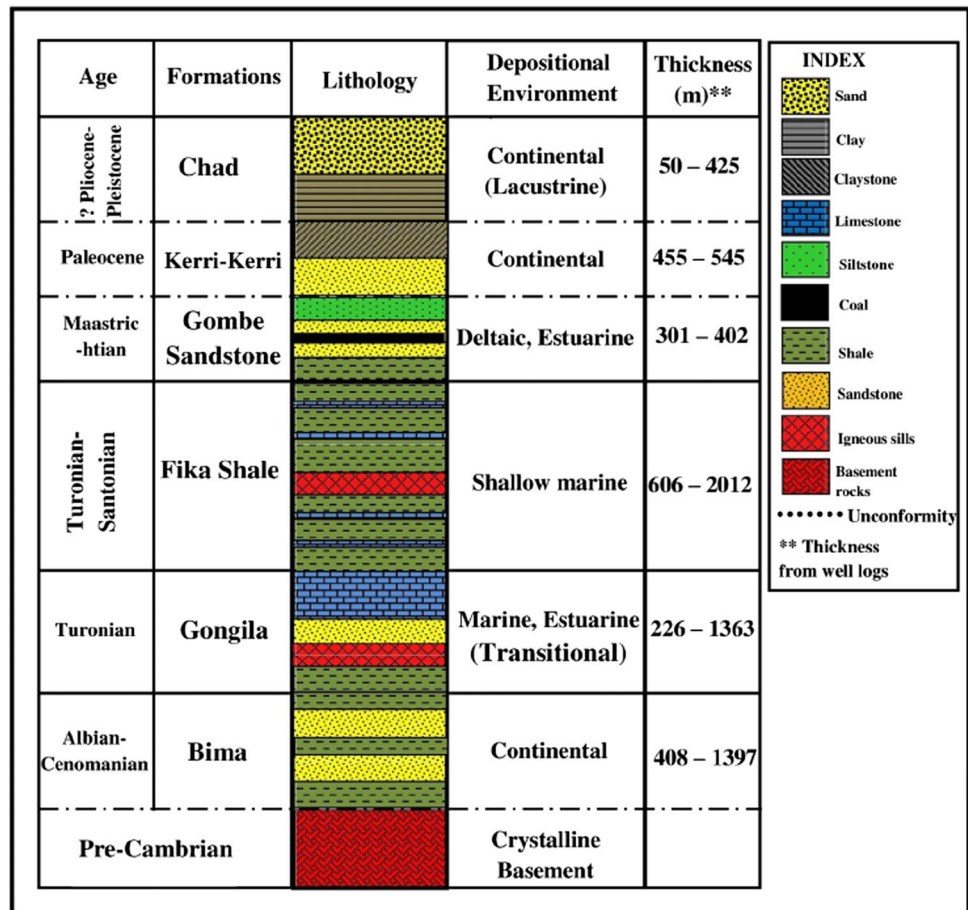
**Basement architecture, topography and estimation of depth to basement**

**Source parameter imaging (SPI)**

The source parameter imaging (SPI) technique, also known as the local wavenumber method, was developed based on the complex analytic signal, which computes source parameters from pre-processing (dx, dy and dz) grids of magnetic data (Thurston and Smith 1997; Thurston et al. 1999 & 2002). The local wavenumber has maxima located over isolated contacts, and depths can be estimated without assumptions about the thickness of the source bodies (Smith et al. 1998). Solution grids using the SPI technique can map the edge locations, depths, dips and susceptibility contrasts. SPI maps resemble geology more closely than the TMI and derivative maps. The



**Fig. 3** Stratigraphic sequence of Bornu Basin (modified after Okosun 1995 and Avbovbo et al. 1986)



depth obtained from SPI is used in oil exploration to determine whether the thickness of sediments is sufficient for hydrocarbon maturation and accumulation. SPI assumes a step-type source model. For a step, the following formula holds:

$$Depth = 1/K_{max} \tag{3}$$

where  $K_{max}$  is the peak value of the local wavenumber  $K$  over the step source.

$$K = \left( \left( \frac{\partial A}{\partial x} \right)^2 + \left( \frac{\partial A}{\partial y} \right)^2 + \left( \frac{\partial A}{\partial z} \right)^2 \right)^{1/2} \tag{4}$$

$$\text{Tilt derivative A} = \tan^{-1} \left( \frac{\frac{dT}{dz}}{\sqrt{\left( \frac{dT}{dx} \right)^2 + \left( \frac{dT}{dy} \right)^2}} \right) \tag{5}$$

**2D modelling of aeromagnetic anomaly**

In the interpretation of magnetic field data, modelling is one of the inverse ways models are generated from which

synthetic magnetic signatures are produced and statistically fitted to the observed data. The amount of information (depth to a particular magnetic body, shape, size and magnetisation) gained from the models developed is determined by the quality and quantity of accessible data, as well as the sophistication of the manual or computer software utilised.

The modelling technique employed in this work is two-dimensional depth modelling produced using the gravity/magnetic system (GM-SYM), an extension modelling interface in Oasis Montaj. The application is an interactive forward modelling programme that calculates the gravity and magnetic response of a hypothetical geologic model defined by the user. Modifying the model structures or attributes eliminates any disparities between the model response and the observed gravity and/or magnetic field (e.g., density or susceptibility of model components). The 2D model can be seen as a series of tabular prisms with axes perpendicular to the profile and blocks and surfaces extending to infinity in the strike direction. These constraints are based on the assumption that the modelled profiles do not change orientation along the length of the model (GETECH 2007).

## Results

### Total magnetic intensity (TMI) and reduced to magnetic equator (RTE) maps

The TMI and TMI-RTE maps of the study area (Figs. 4 and 5) are characterised by varying magnetic signatures, depicting three major anomalies: lithologic units, geologic structures and authigenic minerals in sedimentary rocks (Bird 1997). Figures 4 and 5 were produced in aggregate of colours (red-pink, yellow and green-blue). The red – pink colour depicts positive (high) magnetic anomalies (HMAs) suggesting basement reflection probably an intrusion into the sediments. The presence of this HMA at the extreme southern and southwestern region of the study area might be the response from the porphyritic granite underlying the BF, KF and CF (Fig. 2). The portions on the TMI map with yellowish colour signify moderate magnetic

anomalies (MMAs) suggesting alluvium deposition. While the green-blueish colour depicts low magnetic anomalies (LMAs) attributable to thick sedimentation which is predominant in the study area. The TMI and TMI-RTE values range from  $-151.07$  to  $159.03$  nT and  $-148.13$  to  $150.64$  nT, respectively, and are characterised by long, medium and short-wavelength anomalies. Short-wavelength anomalies dominate the southern flank as a result of the shallow basement. The prominent long-wavelength anomalies in the central-eastern portion of the study area are also conspicuous, reflecting deeper sedimentary piles in CF (Talwani and Walter 2003; Minelli et al. 2018; Wang et al. 2020). The dominant structural features delineated in NE-SW (Figs. 4 and 5) are related to the Pan-African trend (Okosun 1995; Aderoju et al. 2016). On the other hand, the delineated minor structures also trend in ENE-WSW, ESE-WNW, N-S and NW-SE, indicating the traces of different episodes of orogeny in the past (Awoyemi et al. 2022; Okpoli and Akingboye 2020).

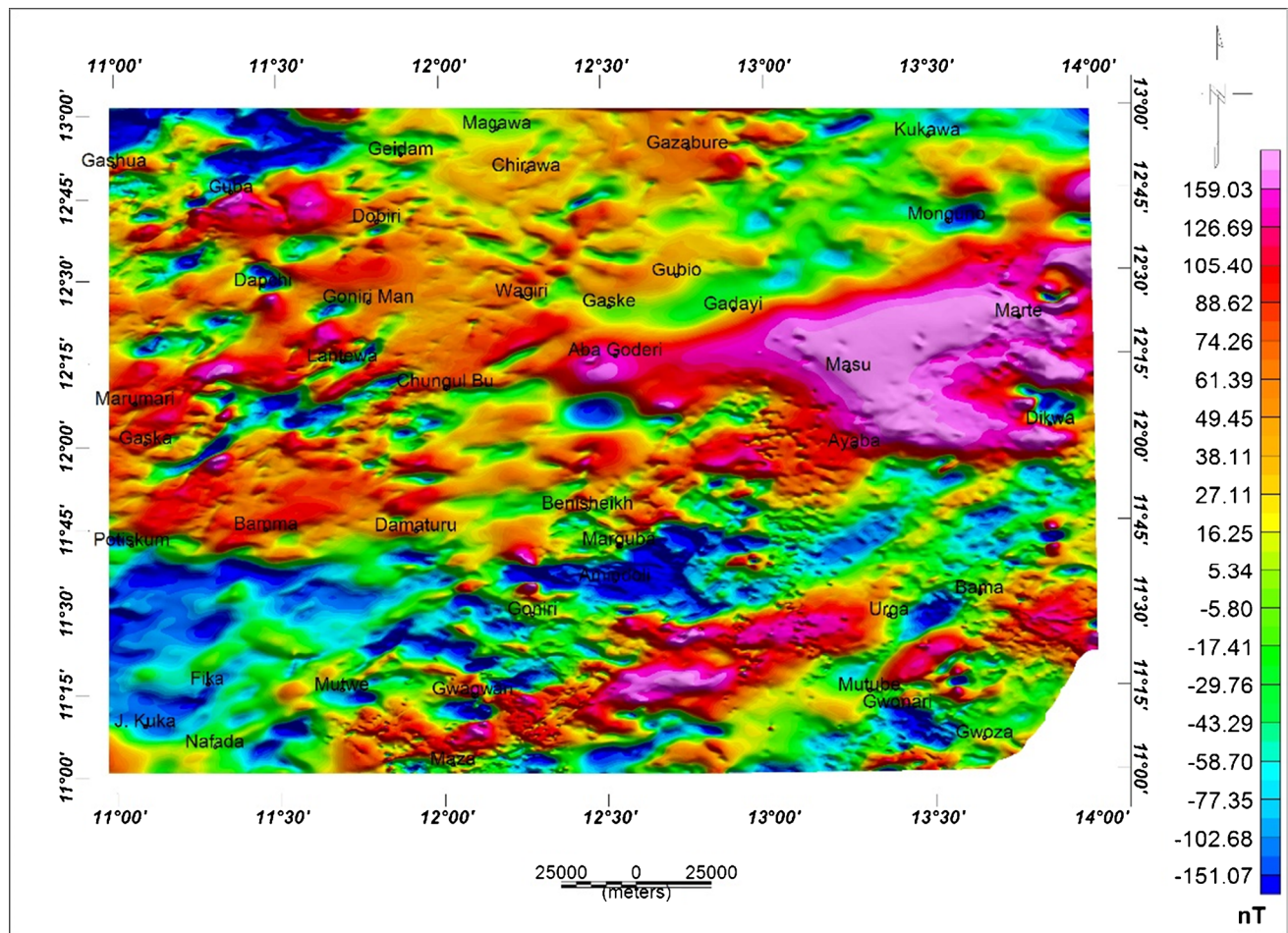


**Fig. 4** Total magnetic intensity map of the study area



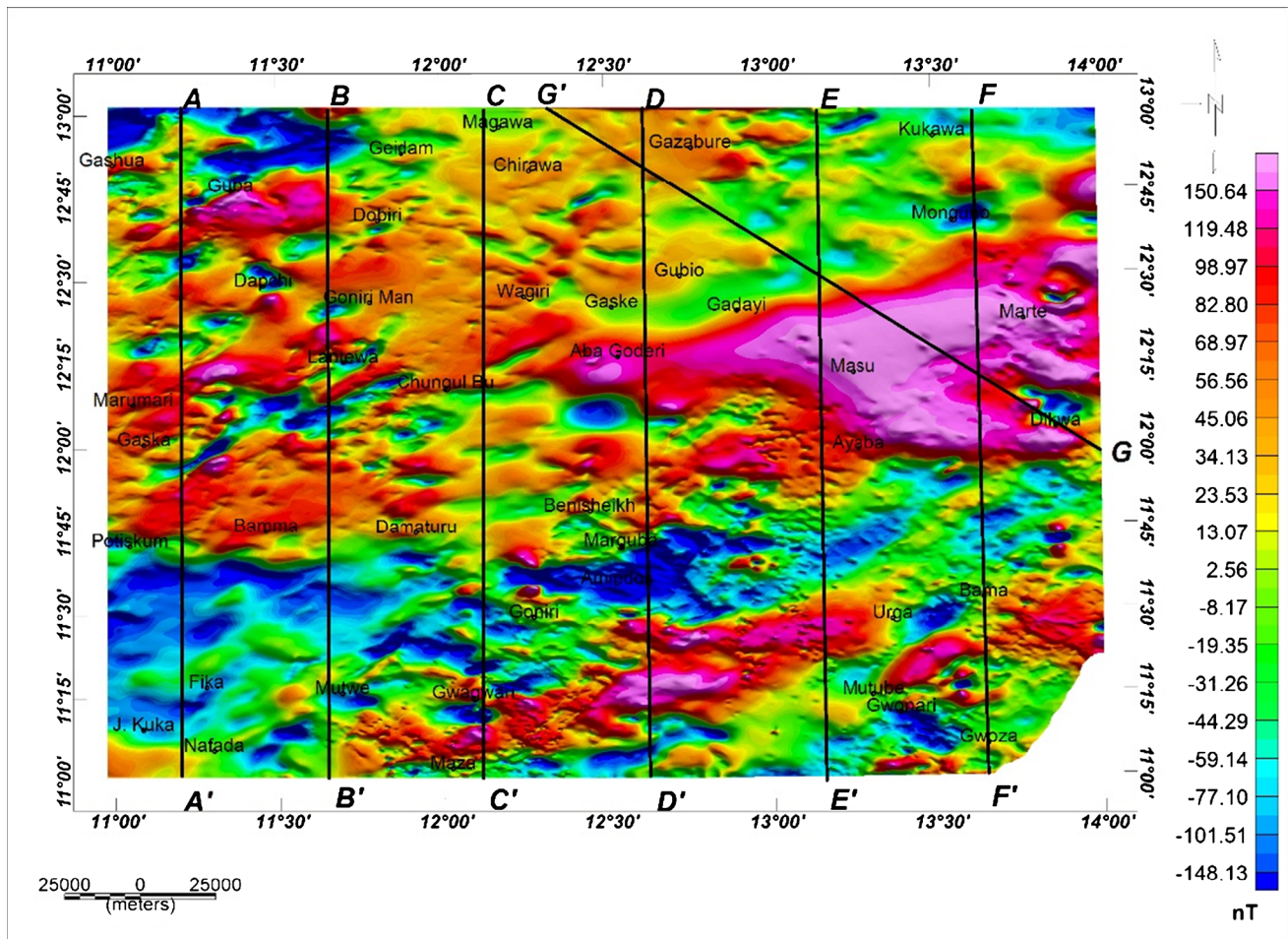


Fig. 5 Reduced to the equator TMI map of the study area

### Discussion

The area under investigation comprises lithological units that include AL (alluvium deposition), CF (Chad Formation), KF (Keri-Keri Formation), GF (Gombe Formation), PF (Pindiga Formation), YF (Yolde Formation) and BF (Bima Formation) (Figs. 2 and 3). The CF is the topmost Pliocene fluvialite and lacustrine sediment, comprising thick clay bodies that separate the three major sand bodies (Wright 1985). The CF dominates the northeastern, central, northwestern and southeastern parts of the study area, accounting for approximately 80% of the study area. It is characterised by high, moderate and low magnetic fields (Figs. 4 and 5). The LMA might be attributable to the influence of Lake Chad in the northeastern portion of the study area. Similarly, the high responses from both magnetic fields could be attributed to thick sediment piles in the study areas (Fig. 5a).

The GF underlies the KF and superimposes the YF in the extreme southwestern region of the study area. The GF comprises intercalations of siltstones, shale and ironstones,

responsible for the observed low magnetization. The PF conformably overlies the YF in the southern part of the study area. It is composed of carbonaceous shales and limestones, intercalated with limestones, shales and minor mudstones, hence responsible for the low to moderate magnetic response. The YF also conformably overlies the BF in the southern part and comprises sandstones, limestones, shales, clays and claystone. The underlying rock, typically medium-grained sandstones intercalated with carbonaceous clays, shales and mudstones, sits unconformably atop the BF (Obaje 2009). The influence of basement rocks enhances the magnetic responses observed in the basin.

### Subsurface geological structures, architecture and crustal thickness

Subsurface geological structures (faults, lineaments) are crucial in hydrocarbon exploration as they help control the migration of oil and gas from the source rocks. The FVD and SVD of RTE-TMI anomalous maps effectively delineate the

geological structures controlling the hydrocarbon accumulation in the study area. The SPI map and the 2D models help in determining the sedimentary thickness and the basement architecture of the study area for hydrocarbon prospecting.

### Vertical derivatives (VDs) and the rose diagram maps

The FVD (Fig. 6a) and SVD (Fig. 6b) are crucial in hydrocarbon exploration as they explicitly delineate geologic structures responsible for the migration of oil and gas from the source rocks. Edge-enhancing magnetic derivative anomaly filters greatly enhanced the high amplitude and short-wavelength (high wavenumber) anomalies associated with the surface to deep-seated intra-sedimentary volcanic rocks (Saada et al. 2021; Pham et al. 2020; Eldosouky et al. 2020). Thus, the occurrences and extents/lateral boundaries of the rock formations within the study area were recognised and mapped. Compared with other sections of the study area, the Aba Goderi, Masu, Marte and Ayaba to Dikwa are characterised by high amplitude CF sediments attributable to the absence of magnetic structures (Fig. 6a). This noticeable feature is characteristic of sedimentary rocks because high magnetic signatures are common for thick sedimentary beds and those with intrusive rocks. However, Fig. 6b shows a few structures at a deeper depth, suggesting a thick sedimentary burial.

The major geological structures delineated in the VD maps (Fig. 6a, b) are categorised into four major parts: the NE-SW, NNE-SSW, ENE-WSW and ESE-WNW, as explicitly shown by the RD (Fig. 6c). The minor structural features, on the other hand, are oriented N-S, WNW-ESE, NW-SE and NNW-SSE. The trends of these geological structures suggest that the area of study might have witnessed several phases of tectonic deformation at different geological times, as explained by Genik (1992) and Okosun (1995). Lesser structures characterise the northeastern and a part of the central portion compared with the remaining parts of the area. This could indicate different burial depths and episodes of structural deformations. These remaining sections, as described above, are probably associated with shallow to moderate depths with interspersed subtle deeper depths from penetrative fractures. Interestingly, the structural trending agrees with the dominated NE-SW trending fault system (Ajakaiye et al. 1986, Avbovbo et al. 1986, and Benkheilil 1988). These structures identified are good migration mechanisms for hydrocarbon in the study area.

### Source parameter imaging (SPI) map

The SPI map of the RTE-TMI of the study area is shown in Fig. 7. The SPI map is characterised by shallow (SD), moderate (MD) and deeper depths (DD). The red-pink colour signifies SD due to a shallow basement, suggesting

insufficient sedimentation for hydrocarbon accumulation and maturation in a sedimentary terrain. The SD ranges from 168.4 to 749.6 m and occupies some areas in the mid-southern, central, southeastern and northwestern regions of the study area, corresponding to the following towns: Yaba, Maza, Doksa, Gwagwari, Goniri, Amindori, Benisheikh, Kumala, Bolori, and Ajiri; Mutube, Gwonari, Bama, Urga, Konduga and Shigaba; Gashua, Kuruawa, Gaska, Mugrum, Marumari, Goniri man, Dobiri, Biri and Lajere, respectively. Likewise, the MD sources ranging from 911.9 to 1554.9 m are attributed to the AL deposition. While the DD sources ranging from 1692.4 to 5554.6 m, signifying thick sedimentation source of about 4500 m, can be observed in the southwestern part (Nafada, J.Kuka, Kadi, Bulako, Fika and Maiduwa). In the mid-eastern part (Hassanari, Aba Goderi, Gaske, Gubio, Gadayi and Masu) and the northeastern part (Monguno and Kukawa), depth sources of 5250 m and 3000 m were obtained, respectively. One of the factors responsible for hydrocarbon generation in a rift basin is the thickness of sediments of 3000 m and above. The thickness of sediment deposits of over 5000 m obtained and discussed above is sufficient for hydrocarbon maturation and accumulation: a good indicator for hydrocarbon prospectivity in the study area. These results agree with some previous studies on parts of the study area (Isogun 2005; Lawal et al. 2007; Chukwunonso et al. 2012; Anakwuba and Augustine 2012; Lawal and Nwankwo 2014; Ajana et al. 2014; Aderoju et al. 2016). The pronounced long-wavelength anomalies in the central flank of the study area observed in Figs. 5 and 6 can clearly be observed on the SPI map (Fig. 7), representing a thick sedimentary pile.

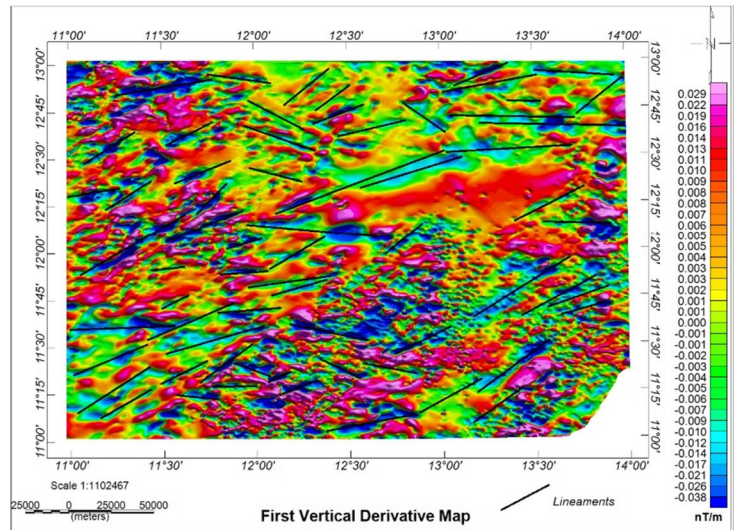
### 2D models of the aeromagnetic anomalies

A 2D model of the aeromagnetic anomalies of the study area was performed to map the subsurface structures, basement topography and basement depth. Seven profiles, A-A', B-B', C-C', D-D', E-E', F-F' and G-G', were carefully selected across significant structures on the TMI-RTE map (Fig. 5). Other data used alongside Fig. 5 were Shuttle Radar Topography Mission (SRTM) for topography enhancement and Fig. 7 for depth control. The terrain clearance used was 100 m, which was added to the SRTM data to obtain the magnetic elevation. Profiles AA<sup>1</sup>-FF<sup>1</sup> (Fig. 8a-f) are 224 km long in the N-S direction, while profile GG<sup>1</sup> (Fig. 8g) is 365 km long in the SE-NW direction. Table 1 presents the summarised results of the 2D magnetic anomaly modelling with respective lithological units, rock compositions and depth to the top of the magnetic basement.

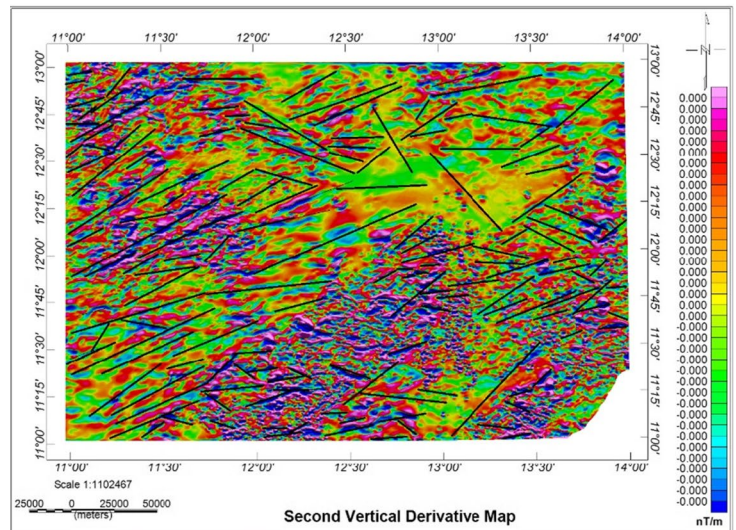
Figure 8a is the model of profile A-A<sup>1</sup>, cutting through the northern AL, the central CF and the southern KF and GF in the study area. It makes the best fit between the calculated and observed anomalies with minimal error.



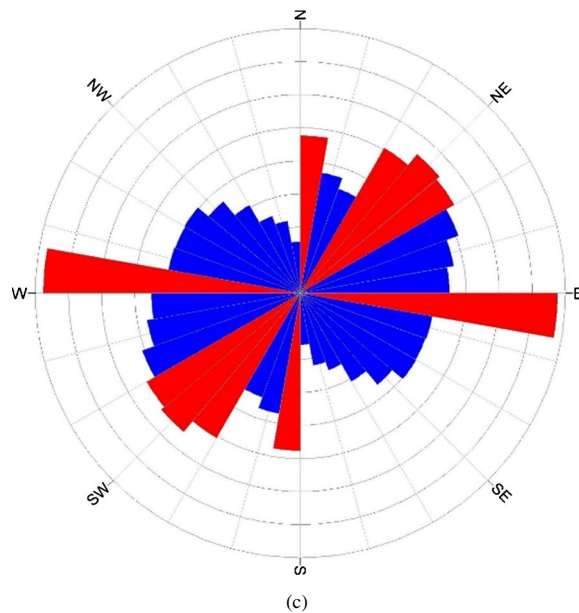
**Fig. 6** **a** First vertical derivative map of the study area, **b** second vertical derivative map of the study area and **c** rose diagram of geological structures within the study area



(a)



(b)



(c)

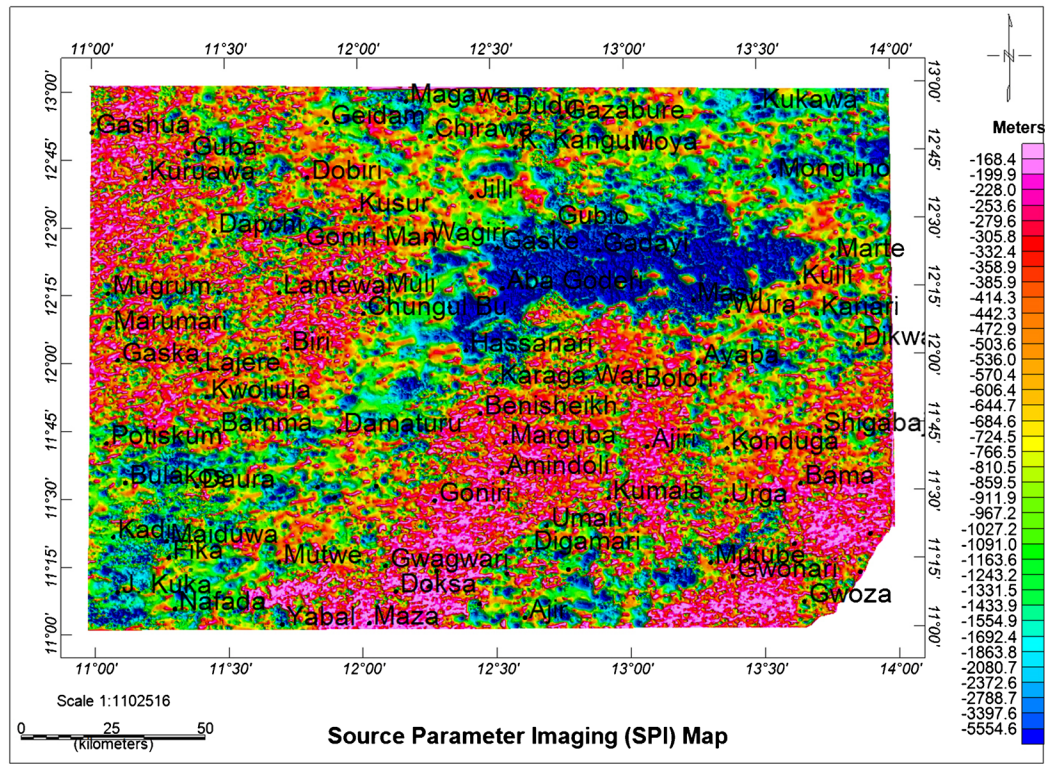


**Fig. 7** Source parameter imaging (SPI) map of the study area

Figure 8a reveals sedimentation of 1 km in the northward region corresponding to Gashua within the AL. Also, towards the central region, a depression of ~120-km distance was observed with sedimentation piles of >3.0 to 4.8 km, corresponding to Fulatari, Gaske and Gabdam within the CF. Towards the southern region, the basement uplifts into the sediments limiting the sediment thickness to ~1.0 km, corresponding to Jangadoli within the KF in the southwestern part of the study area. Likewise, towards the extreme southern region corresponding to GF, a slight depression was also observed to a thickness of 3.0 km. Overall, the thickness of sediments obtained from this model ranges from 1 to 4.8 km. The maximum thickness of sediments of 3.0 to 4.8 km in the central region of Figs. 7 and 8a, corresponding to Fulatari, Gaske and Gabdam, is enough for hydrocarbon maturation and accumulation. Figure 8a also reveals an undulated basement topography and a contrast in magnetic susceptibility and magnetization, with sediment having 0.0 magnetic susceptibility and basement rock having magnetic susceptibility and magnetization of 0.003 and 0.002, respectively.

Figure 8b is the model of profile B-B<sup>1</sup> that cuts across the AL, CF, PF and YF in the north, central and southern parts of the study area, respectively. In the northern part, the model (Fig. 8b) reveals a depth to the top of the basement of 1.0 km. Likewise, 15 km away from the northern region, a depression of 4.0-km depth was observed, which

continued towards the central part, maintaining the same depth to about 120-km distance in the CF. Also, a shallow basement of 1 km deep towards the southern part of PF was observed. On the other hand, a slight depression of ~2.0 km within the PF and YF was noticed. The highest sedimentary thickness of 4.0 km towards the central region of the model (Fig. 8b) corresponds to the following locations: Lantewa, Biriri, Gabai, Alagarnoi, Garin and Basam, which is enough for hydrocarbon maturation and accumulation to take place..

Similarly, the modelled profile C-C' (Fig. 8c) cut through the AL and CF in the northern to the central parts of the study area, as well as the GF and underlying basement in the south. Unlike Fig. 8a, b, this model (Fig. 8c) shows a thickness of sediments of 2.0 km deep at a distance of 65 km from the north to the central region, with a slight depression of about 20 km long and 2.6 km deep within the CF. An undulating basement uplift into the sediments of about 80 km long and 1.0 to 1.8 km deep was observed towards the southern region of the study area within the GF. The uplift observed was a result of basement intrusion into the CF and underlain by the GF, and this can be attributable to the presence of the underlying basement in the southern region of the study area (Fig. 2).

Likewise, Fig. 8d represents the model of profile D-D', which cuts across the CF from the northern part to the central part and, towards the southern region, enters into the

**Fig. 8** Two-dimensional models of profiles: **a** A-A' in N-S, **b** B-B' in N-S, **c** C-C' in N-S, **d** D-D' in N-S, **e** E-E' in N-S, **f** F-F' in N-S and **g** G-G' in SE-NW directions generated from the RTP-TMI map of the study area

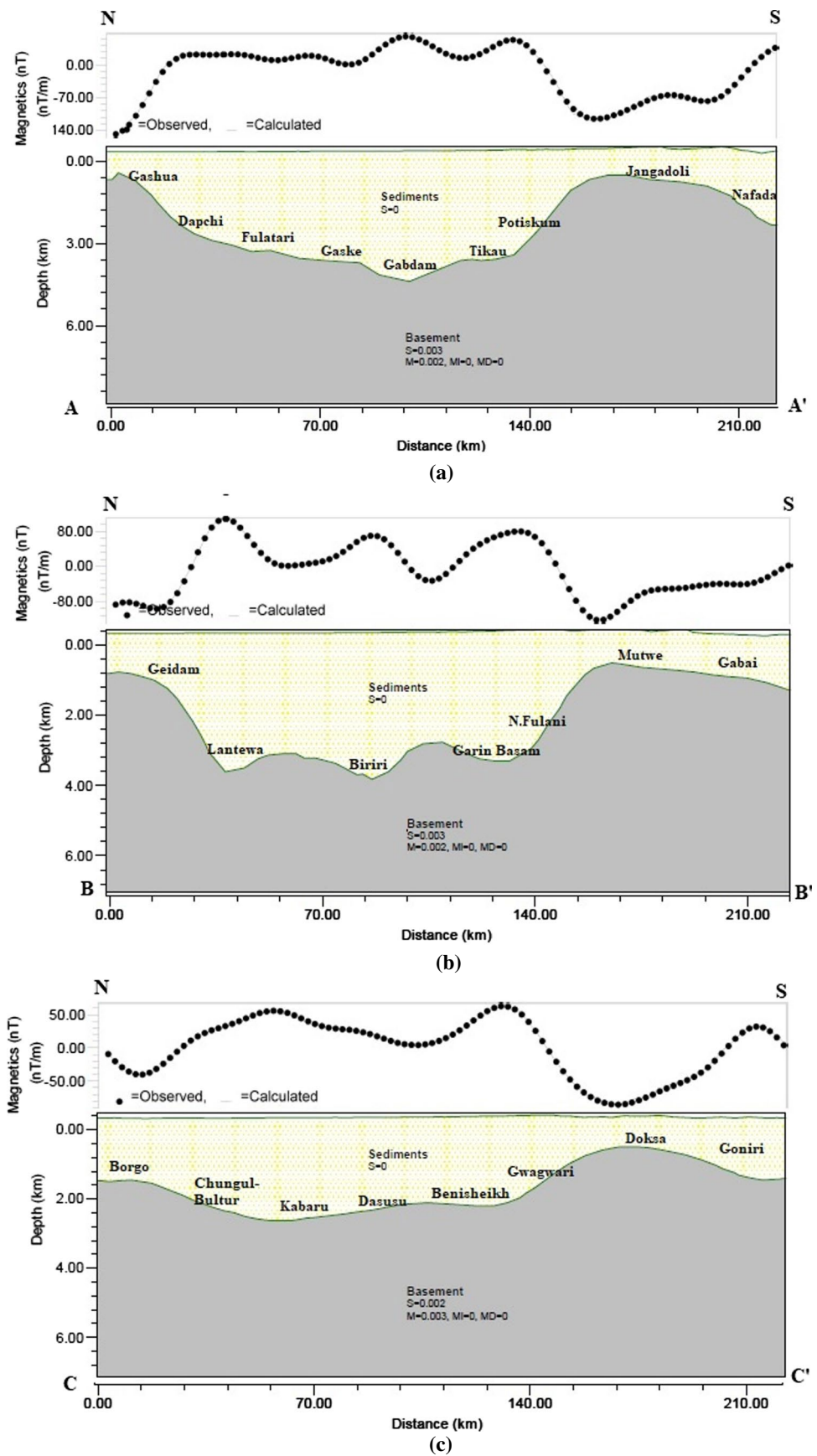




Fig. 8 (continued)

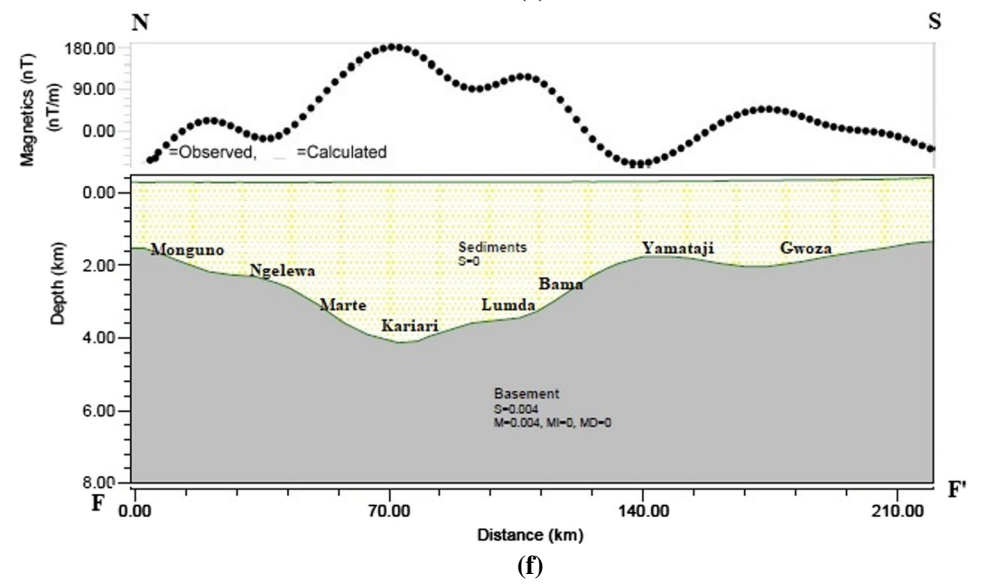
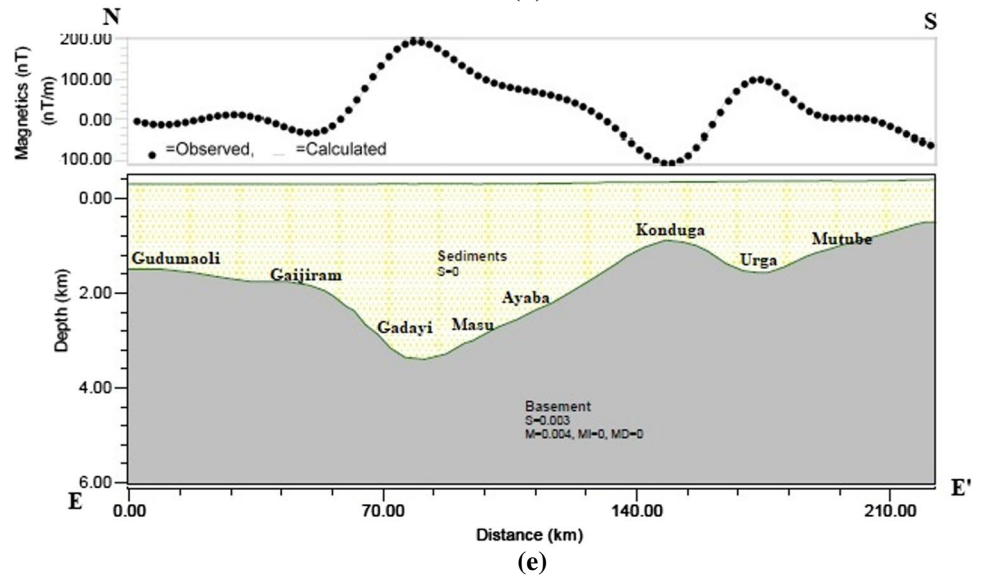
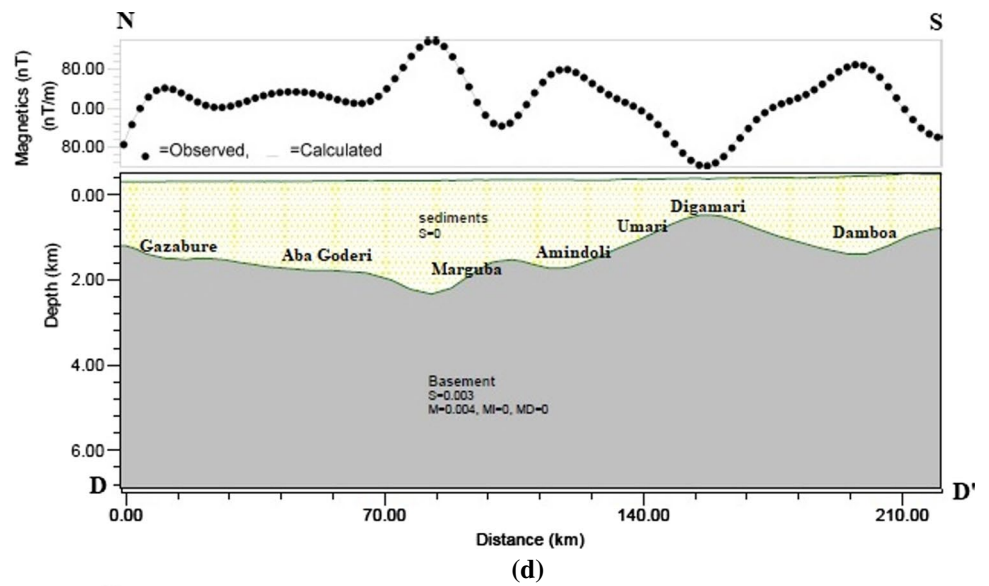
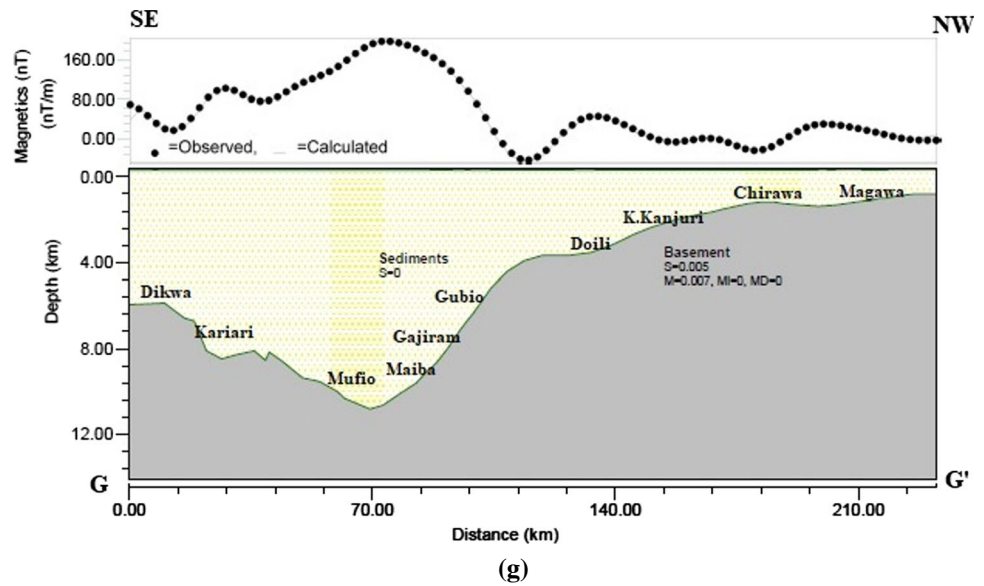




Fig. 8 (continued)



**Table 1** Summary of the 2D magnetic anomaly modelling with respective lithological units, rock formations and depths

S/N	Profile name	Profile directions	Profile distance (km)	Lithological units	Rock composition	Depth to top of the basement (km)	Probable hydro-carbon potential remarks
1	A-A'	N-S	224 km	AL	Sandstones	> 1.0 km	No
				CF	Thick clay	3.0–4.8 km	Yes
				KF	Sandstones, clay and claystones	> 1.0 km	No
				GF	Siltstones, shale and ironstones	3 km	Yes
2	B-B'	N-S	224 km	AL	Sandstones	> 1.0 km	No
				CF	Thick clay	3.2–4.0 km	Yes
				PF	Limestones, shale, mudstones	> 1.0 km	No
				YF	Sandstones, limestones, clay and claystones	> 2.0 km	No
3	C-C'	N-S	224 km	AL	Sandstones	> 2.0 km	No
				CF	Thick clay	> 2.6 km	Yes
				GF	Siltstones, shale and ironstones	< 2.0 km	No
				Basement rock	Porphyritic granite	1.0 km	No
4	D-D'	N-S	224 km	CF	Thick clay	> 2.6 km	Yes
				KF	Sandstones, clay and claystones	< 2.0 km	No
				BF	Clay, mudstones and shale	< 2.0 km	No
				Basement rock	Porphyritic granite	> 1.0 km	No
5	E-E'	N-S	224 km	CF	Thick clay	> 2.0–4.0 km	Yes
				KF	Sandstones, clay and claystones	> 2.0 km	Yes
				Basement rock	Porphyritic granite	> 1.0 km	No
6	F-F'	N-S	224 km	CF	Thick clay	2–> 4.0 km	Yes
				Basement rock	Porphyritic granite	> 1.0 km	No
				AL	Sandstones	2.0 km	No

KF and BF. Similar to Fig. 8c, Fig. 8d shows a depth of 2.0 km at a distance of 65 km from the north towards the central region within the CF. In the central portion corresponding to Marguba, a slight depression of about 20 km

long and 2.6 km deep was also noticed within the CF. On the other hand, an undulating uplift of the basement into the sediments of about 80 km long and 1.0 to 1.8 km deep was observed towards the southern region of the study area

within the KF. This uplift might be due to the shallow basement in the southern part of the study area. In general, the thickness of sediments obtained from this model (Fig. 8d) ranges from 0.00 to 26 km, suggesting a shallow basement.

Figure 8e, the model of profile E-E<sup>1</sup>, cuts across the CF from the northern region to the central region of the study area and enters into the KF and the underlying basement in the southern part of the study area. This model comprises two lithologic units: the sedimentary and the basement section. A sediment thickness of 2.0 km was measured over a distance of 54 km in the northern part of the CF, corresponding to Gudumaoli and Gajjiram, and in the central part, corresponding to Gadayi and Masu. Also, a depression of 4.0 km deep with a distance of 82 km long, a shallow basement of 1.7 km and a distance of 15 km in the southern part were recorded. Likewise, a slight depression was noticed with a depth of 2.0 km and a length of 28 km corresponding to Urga within the KF and then a shallow basement due to porphyritic granite intrusion into the sediments in the southern region of the study area. A sedimentary thickness of 4.0 km obtained at the central part of this model (Fig. 8e) is sufficient for hydrocarbon maturation.

Figure 8f presents the model of the profile F-F<sup>1</sup> that cuts across the CF from the north through the central part and towards the southern region before entering the underlying basement (porphyritic granite) at the extreme southern region of the study area. The model (Fig. 8f) produces the best match between the observed and calculated anomalies with the minimum error recorded. It reveals a mirror reflection of the basement topography. A depth to the top of the basement of 2.0 to 3.0 km with a distance of 60 km was recorded in the northern part of the study area corresponding to Monguno and Ngelewa, and towards the central region of the study area corresponding to Marte, Kariari and Lumda, a depression of over 4.0 km deep and 85 km long was observed. Also, an uplift to a depth of 2.0 km was observed towards the southern region corresponding to Yamataji, caused by the basement intrusion into the sediments attributable to the porphyritic granite at the extreme southern part of the study area. In the central region, a maximum thickness of 4.0 km was recorded, and it was shallow in the southern part of the study area. This model shows a good correlation with the geologic map of the study area. Magnetic susceptibility of 0.0 was recorded for the sedimentary region and 0.004 for the basement region.

The model (Fig. 8g) for profile G-G<sup>1</sup> was carefully taken in a SE-NW direction across a very deep, profound anomaly on the RTE-TMI map (Fig. 5) in the central-eastern part of the study area. Figure 8g cuts across the CF in the eastern part and the AF in the northern part of the study area. In the extreme eastern part of the model corresponding to Dikwa, a thick sedimentary pile of 5.5 km was observed. Also, in the mid-eastern part corresponding to Mufio and Maiba, a

very large depression of almost 11.5 km deep and 120 km long was observed, and a basement depth of 5.0 km deep and 100 km long was recorded towards the central northern part of the study area corresponding to Gubio within the CF. And finally, at the northern part of the AF, a depth of 2.0 km was obtained. So far, no depth of 11.5 km has been recorded along the same anomaly using other depth estimating techniques such as the spectral depth method, SPI and Euler deconvolution by different workers who have worked in the area before (Isogun 2005; Lawal et al. 2007; Chukwunonso et al. 2012; Anakwuba and Chinkwuko 2012; Lawal and Nwankwo 2014; Ajana et al. 2014; Aderoju et al. 2016). Even in this study, the SPI methods employed give the highest depth of 5.7 km along the same anomaly. Ramadas et al. (2004) acknowledged the fact that some depth estimating methods, such as the spectral depth method, SPI and Euler deconvolution, suffer from various impediments because of their inability to map the undulating basement accurately as they only provide average depths. This clarifies why the 2D forward modelling was employed to provide the thickness of sediments and accurately mirror the basement topography in this study. Hence, a thickness of almost 12 km was depicted by the 2D magnetic models for this study (Fig. 8g). This correlates to the thickness of sediments obtained at the Termit basin in the southeastern part of Niger, which has similar geological features to the study area (Genik 1993).

In summary, this study reveals major geological structures in NE-SW, NNE-SSW, ENE-WSW and ESE-WNW that might control the migration of oil and gas within the study area. The thickness of sediments of over 5.0 km obtained in the eastern part of the study area corresponding to Dikwa is in contrast to the previous study carried out by Anakwuba et al. (2011), where the thickness of sediments obtained was 2.7 km in the same area. The 2D models reveal a thickness of sediments ranging from 1.0 to 11.5 km. The maximum thickness of sediments of 3.0 to 11.5 km obtained in CF and GF is sufficient for hydrocarbon maturation and accumulation in a rift basin. The potential hydrocarbon spots of the area investigated are presented in the contour map in Fig. 9, depicting sections with a thickness of 3.0 km and above as good sources which might be rich in hydrocarbon accumulation. These rich hydrocarbon spots are located in the central, the west, the northeast, the southwest, the central-eastern and the eastern parts, corresponding to Gubio, Gabdam, Monguno, Nafada, Gadabayi and Dikwa areas. Likewise, Fig. 10 shows the estimated depth to the top of magnetic basement topography digitized from depth models (Fig. 8a–g). The 3D surface map (Fig. 10) revealed an undulating basement and a subsidence in the eastern flank of the study area confirming the deep-seated structure delineated in Figs. 4 and 5. The common uplifts delineated on the model AA<sup>1</sup>-FF<sup>1</sup> at latitude 11.25°N might be evidence of the boundary between the Chad formation and its adjoining

**Fig. 9** Hydrocarbon prospectivity map showing the summary of regions of high and low hydrocarbon potential spots in the study area

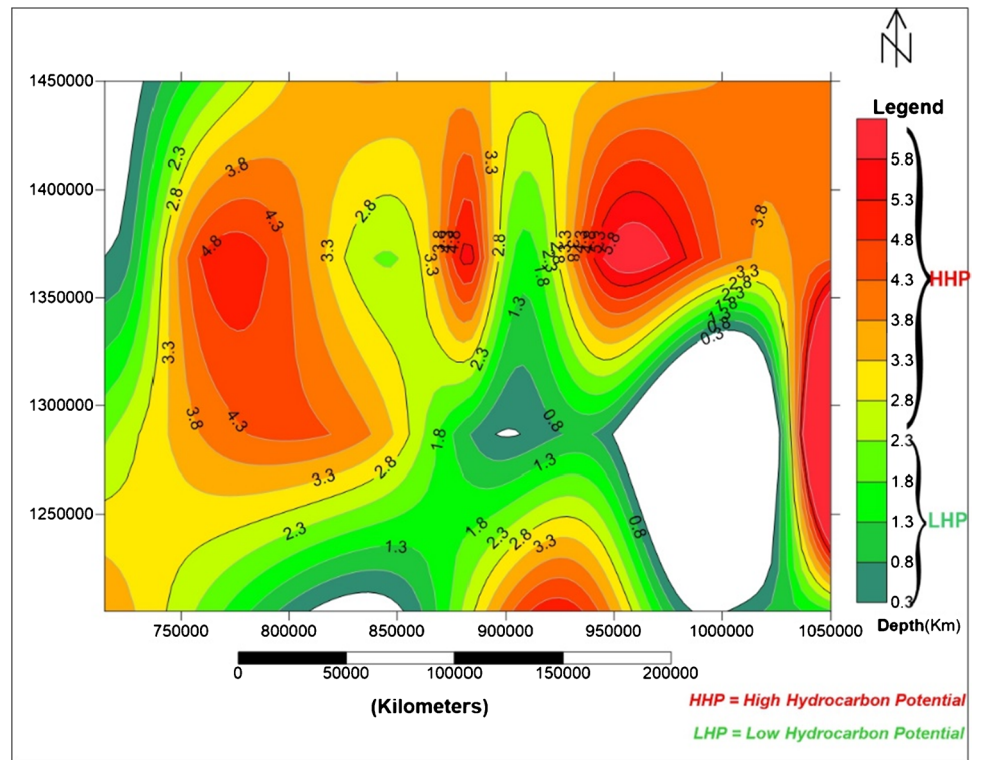
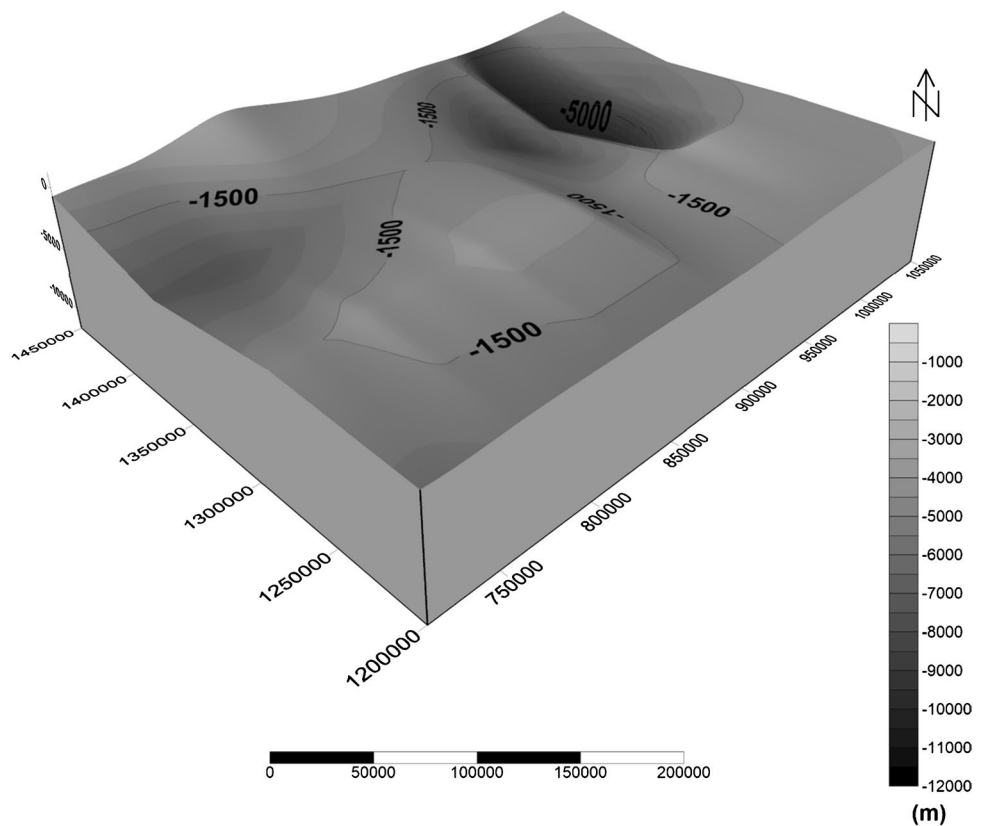


**Fig. 10** Three-dimensional surface map of depth to the top of basement topography



Gongola basin in the Upper Benue Trough, as explained by Zaborski et al. (1998) and Salako and Udensi (2015). The 2D modelling and the SPI results are correlated to some extent, apart from the central-eastern part with a thickness of 11.5 km (Fig. 8g). The two results correspond with some previous studies (Isogun, 2005; Lawal et al. 2007; Chukwunonso et al. 2012; Anakwuba and Chinkwuko 2012; Lawal and Nwankwo 2014; Ajana et al. 2014; Aderoju et al. 2016) and the Termit basin in the southeastern part of the Niger Republic with  $\approx 12$  km sediment thickness (Genik 1993). Similarly, the gravity modelling of the Chad basin shows the extent and thickness of the Cretaceous-Tertiary rift basin ranging from about 3 to  $> 12$  km (Genik 1992 & 1993 and Zanguina et al. 1998).

## Conclusion

This study has successfully mapped the subsurface geological structures and thickness of sediments from vertical derivatives, SPI and 2D magnetic modelling of magnetic anomaly data of the Bornu Basin and its environs for possible hydrocarbon generation and accumulation. The results revealed the varying lithological and shallow-to-deep structural (faults and lineaments) features and the trending of the structures. These characteristic geologic features depicted varying magnetic fields. The high anomalous field, with a long wavelength observed in the central-eastern part of the study area, suggests a thick sedimentary pile. The FVD, SVD and RD show the major geological structures migrating or trapping oil and gas trends in NE-SW, NNE-SSW, ENE-WSW and ESE-WNW directions in the study area. The SPI reveals a shallow depth of 168.4–749.6 m, a moderate depth of 911.9–1554.9 m and deeper depths of 1692.4–5554.6 m. Also, the 2D magnetic anomaly modelling reveals an undulating basement underlying the sediments, with a depth range of 1.0 to 11.5 km. The thickness of 3.0 km and above sediments obtained from this study falls within the oil window in a Cretaceous-Tertiary rift basin in the mega Chad Basin. Therefore, the study's findings have provided significant insights into the subsurface structural architecture of the Bornu Basin for hydrocarbon prospecting.

## Declarations

**Conflict of interest** The authors declare no competing interests.

## References

- Abubakar MB (2014) Petroleum potentials of the Nigerian Benue Trough and Anambra Basin: a regional synthesis. *Nat Resour* 5(1):25–58. <https://doi.org/10.4236/nr.2014.5100>
- Aderoju AB, Ojo SB, Adepelumi AA, Edino F (2016) A reassessment of hydrocarbon prospectivity of the Chad basin, Nigeria, using magnetic hydrocarbon indicators from high-resolution aeromagnetic imaging. *Ife J Sci* 18(2):503–20
- Adeyemi T, Salako KA (2018) Delineation of mineral potential zone using high resolution aeromagnetic data over part of Nasarawa State, North Central, Nigeria. *Egypt J Pet* 27(4):759–767
- Adeyemi T, Salako KA, Usman AD, Udensi EE (2021) Heat flow analyses over Bornu Basin and its environs, Northeast Nigeria, using airborne magnetic and radiometric data: implication for geothermal energy prospecting. *Arab J Geosci* 14(14):1–19
- Adeyemi T, Salako KA, Salami MK, Mohammed MA, Udensi, EE (2017) Estimation of sedimentary thickness using spectral analysis of aeromagnetic data over part of Bornu Basin, Northeast, Nigeria. *Asian J Phys Chem Sci* 1–8
- Ahmed KS, Liu K, Moussa H, Liu J, Ahmed HA, Kra KL (2022) Assessment of petroleum system elements and migration pattern of Borno (Chad) Basin, northeastern Nigeria. *J Petrol Sci Eng* 208:109505
- Ajakaiye DE, Award MB, Ojo SE, Hall DH, Miller TW (1986) Aeromagnetic anomalies and tectonics trends in and around the Benue. *Nature* 319:582–584
- Ajana O, Udensi EE, Momoh M, Rai JK, Muhammad SB (2014) Spectral depths estimate of subsurface structures in parts of Borno Basin, Northeastern Nigeria, using aeromagnetic data. *IOSR J Appl Geol Geophys* 2(2):55–60
- Akanji AO, Sanuade OA, Osinowo OO, Okafor OI (2020) Interpretation of high resolution aeromagnetic data for hydrocarbon exploration in Bornu Basin, Northeastern, Nigeria. *Ann Geophys* 63(2):GM222–GM222
- Akiishi M, Udochukwu BC, Tyovenda AA (2019) Determination of hydrocarbon potentials in Masu area in northeastern Nigeria using forward and inverse modeling of aeromagnetic and aerogravity data. *SN Appl Sci* 1(8):1–15
- Anakwuba EK, Onwumesi AG, Chinwuko AI, Onuba LN (2011) The interpretation of aeromagnetic anomalies over Maiduguri-Dikwa depression, Chad Basin, Nigeria: a structural review. *Arch Appl Sci Res* 3(3):1757–1766
- Anakwuba EK, Chinkwuko A (2012) Re-evaluation of hydrocarbon potential of Eastern Part of the Chad Basin, Nigeria: an aeromagnetic approach. *Search and Discovery Article* 2(1):78–90
- Anudu GK, Stephenson RA, Macdonald DI (2014) Using high-resolution aeromagnetic data to recognise and map intra-sedimentary volcanic rocks and geological structures across the Cretaceous middle Benue Trough, Nigeria. *J Afr Earth Sci* 1(99):625–636
- Arogundade AB, Hammed OS, Awoyemi MO, Falade SC, Ajama OD, Olayode FA, Olabode AO (2020) Analysis of aeromagnetic anomalies of parts of Chad Basin, Nigeria, using high-resolution aeromagnetic data. *Model Earth Syst Environ* 6(3):1545–1556
- Avbovbo AA, Ayoola EO, Osahon GA (1986) Depositional and structural styles in Chad Basin of northeastern Nigeria. *Bull Am Assoc Pet Geol* 70:1787–1798
- Awoyemi MO, Falade SC, Arogundade AB, Hammed OS, Ajama OD, Falade AH, Adebisi LS, Dopamu KO, Alejelowo EA (2022) Magnetically inferred regional heat flow and geological structures in parts of Chad Basin, Nigeria and their implications for geothermal and hydrocarbon prospects. *J Petrol Sci Eng* 213:110388
- Benkhelil J (1988) Structure et Evolution Geodynamique du Bassin Intracontinental de la Benue (Nigeria). *Bul Cent Rech Explor-Prod Elf-Aquitaine* 12:29–128
- Bird DE (1997) Primer: interpreting magnetic data. *Am Assoc Pet Geol Explor* 8(5):18–21
- Biswas M, Puniya MK, Gogoi MP, Dasgupta S, Mukherjee S, Kar NR (in press) Morphotectonic analysis of petroliferous Barmer rift basin (Rajasthan, India). *J Earth Syst Sci*



- Chukwunonso OC, Godwin OA, Kenekukwu AE, Ifeanyi CA, Emmanuel IB, Ojonugwa UA (2012) Aeromagnetic interpretation over Maiduguri and environs of Southern Chad Basin, Nigeria. *J Earth Sci Geotech Eng* 2(3):77–93
- Cooper GR, Cowan DR (2004) Filtering using variable order vertical derivatives. *Comput Geosci* 30(5):455–459
- Dasgupta S, Mukherjee S (2017) Brittle shear tectonics in a narrow continental rift: asymmetric non-volcanic Barmer basin (Rajasthan, India). *J Geol* 125:561–591
- Dasgupta BM, Mukherjee S, Chatterjee R (2022) Structural evolution and sediment depositional system along the transform margin-Palar-Pennar basin, Indian east coast. *J Petrol Sci Eng* 211:110155
- Dasgupta S, Mukherjee S (2019) Remote sensing in lineament identification: examples from western India. In: Billi A, Fagereng A (Eds) *Problems and Solutions in Structural Geology and Tectonics*. Developments in Structural Geology and Tectonics Book Series. Vol 5. Series Editor: Mukherjee S. Elsevier. ISSN: 2542–9000
- Ekwok SE, Achadu OIM, Akpan AE, Eldosouky AM, Ufuafuonye CH, Abdelrahman K, Gómez-Ortiz D (2022) Depth estimation of sedimentary sections and basement rocks in the Bornu Basin, Northeast Nigeria using high-resolution airborne magnetic data. *Minerals* 12(3):285
- Ekwok SE, Akpan AE, Kudamnya EA (2020) Exploratory mapping of structures controlling mineralization in Southeast Nigeria using high resolution airborne magnetic data. *J Afr Earth Sci* 162:103700
- Eldosouky AM, Elkhateeb SO, Ali A, Kharbush S (2020) Enhancing linear features in aeromagnetic data using directional horizontal gradient at Wadi Haimur area, South Eastern Desert, Egypt. *Carpathian J Earth Environ Sci* 15(2):323–6
- Eldosouky AM, El-Qassas RA, Pour AB, Mohamed H, Sekandari M (2021) Integration of ASTER satellite imagery and 3D inversion of aeromagnetic data for deep mineral exploration. *Adv Space Res* 68(9):3641–3662
- Eldosouky AM, Pham LT, Abdelrahman K, Fnais MS, Gomez-Ortiz D (2022) Mapping structural features of the Wadi Umm Dulfah area using aeromagnetic data. *Journal of King Saud University-Science* 34(2):101803
- Elkhateeb SO, Eldosouky AM, Khalifa MO, Aboalhassan M (2021) Probability of mineral occurrence in the Southeast of Aswan area, Egypt, from the analysis of aeromagnetic data. *Arab J Geosci* 14:1514
- Emujakporue G, Nwankwo C, Nwosu L (2012) Integration of well logs and seismic data for prospects evaluation of an X field, onshore Niger Delta, Nigeria. *Int J Geosci* 3:872–877
- Genik GJ (1992) Regional framework, structural and petroleum aspects of rift basins in Niger, Chad and the Central African Republic (C.A.R.). *Tectonophysics* 213:169–185
- Genik GJ (1993) Petroleum geology of the Cretaceous-Tertiary Rift Basins in Niger, Chad and the Central African Republic. *Bull Am Assoc Pet Geol* 77:1405–1434
- GETECH Group Plc (2007) Advanced processing and interpretation of gravity magnetic data. GETECH (Geophysical Exploration and Technology) Group Plc. Kitson house Elmets hall leeds, UK 22p
- Guiraud R, Binks RM, Fairhead JD, Wilson M (1992) Chronology and geodynamic setting of Cretaceous-Cenozoic rifting in West and Central Africa. *Tectonophysics* 213(1–2):227–234
- Isogun MA (2005) Quantitative interpretation of aeromagnetic data of Chad Basin, Bornu State, Nigeria. Unpublished. M.sc. Thesis, O.A.U Ile-Ife
- Isyaku AA, Rust D, Teeuw R, Whitworth M (2016) Integrated well log and 2-D seismic data interpretation to image the subsurface stratigraphy and structure in northeastern Bornu (Chad) basin. *J Afr Earth Sc* 121:1–15
- Kar NK, Mani D, Mukherjee S, Dasgupta S, Puniya MK, Kaushik AK, Biswas M, Babu EVSSK (2022) Source rock properties and kerogen decomposition kinetics of Eocene shales from petroliferous Barmer basin, western Rajasthan, India. *J Nat Gas Sci Eng* 100:104497
- Lawal TO, Nwankwo LI (2014) Wavelet analysis of high resolution aeromagnetic data over part of Chad Basin, Nigeria. *Ilorin J Sci* 1:110–120
- Lawal KM, Umego MN, Ojo SB (2007) Depth-to-basement mapping using fractal technique: application to the Chad Basin, North-eastern Nigeria. *Nigerian J Phys* 19(1):75–88
- Lawal TO, Nwankwo LI, Akoshile CO (2015) Wavelet analysis of aeromagnetic data of Chad Basin, Nigeria. *Afr Rev Phys* 10:0016
- Melouah O, Eldosouky AM, Ebong ED (2021) Crustal architecture, heat transfer modes and geothermal energy potentials of the Algerian Triassic provinces. *Geothermics* 96:102211
- Minelli L, Speranza F, Nicolosi I, D’Ajello Caracciolo F, Carluccio R, Chiappini S, Messina A, Chiappini M (2018) Aeromagnetic investigation of the central Apennine Seismogenic Zone (Italy): from basins to faults. *Tectonics* 37:1435–1453. <https://doi.org/10.1002/2017TC004953>
- Nabilou M, Afzal P, Arian M, Adib A, Kheyrollahi H, Foudazi M, Ansarirad P (2022) The relationship between Fe mineralization and magnetic basement faults using multifractal modeling in the Esfordi and Behabad Areas (BMD), Central Iran. *Acta Geologica Sinica-English Edition* 96(2):591–606
- Nigerian Geological Survey Agency (NGSA) (2005) Newsletter
- Obaje NG (2009) *Geology and mineral resources of Nigeria*. Lecture Notes in Earth Sciences. Springer, Berlin Heidelberg
- Obaje NG, Wehner H, Scheeder G, Abubakar MB, Jauro A (2004) Hydrocarbon prospectivity of Nigeria’s inland basins: from the viewpoint of organic geochemistry and organic petrology. *AAPG Bull* 87:325–353
- Ogunbesan G, Adedosu, T, Raji M (2020) Petroleum potential of late Cretaceous shale of Wadi-1 Well, Chad Basin, Northeastern Nigeria. In: 82nd EAGE Annual Conference & Exhibition. 2020(1):1–5
- Okosun EA (1992) Cretaceous ostracod biostratigraphy from Chad basin in Nigeria. *J Afr Earth Sci* 14(3):327–339
- Okosun EA (1995) Review of the geology of Bornu Basin. *J Min Geol* 31:113–122
- Okpikoro EF, Olorunniwo MA (2010) The application of seismic-log sequence stratigraphy in mapping stratigraphic traps and reservoirs’ facies in Afam channel area, Niger Delta. *Glob J Geol Sci* 8(1)
- Okpoli CC, Akingboye AS (2020) Application of airborne gravimetry data for litho-structural and depth characterisation of Precambrian Basement Rock (Northwestern Nigeria). *Geophysica* 55:3–21
- Ola PS (2018) Source rock evaluation of the shale beds penetrated by Kinasar-1 Well, Se Bornu Basin, Nigeria. *Open J Geol* 8(11):1056
- Olubode SO, Adekoya JA, Ola PS (2015) Distribution of sedimentary formations in the Bornu Basin, Nigeria. *Pet Explor Dev* 42(5):674–682
- Olugbemiro RO, Ligouis B, Abaa SI (1997) The Cretaceous series in the Chad Basin, NE Nigeria: source rock potential and thermal maturity. *J Petrol Geol* 20:51–68
- Pham LT, Eldosouky AM, Oksum E, Saada SA (2020) A new high resolution filter for source edge detection of potential field data. *Geocarto Int* 17:1–8
- Ramadas G, Himabindu D, Ramaprasada IB (2004) Magnetic basement along the Jadcharla–Vasco transect, Dharwar craton India. *Curr Sci* 86(11):1548–1553
- Razavi Pash R, Davoodi Z, Mukherjee S, Hashemi-Dehsarvi L, Ghasemi-Rozveh T (2021) Interpretation of aeromagnetic data to detect the deep-seated basement faults in fold thrust belts: NW part of the petroliferous Fars province, Zagros belt, Iran. *Mar Pet Geol* 133:105292

- Saada SA, Mickus K, Eldosouky AM, Ibrahim A (2021) Insights on the tectonic styles of the Red Sea rift using gravity and magnetic data. *Mar Pet Geol* 1(133):105253
- Saada SA, Eldosouky AM, Kamel M, El Khadragy A, Abdelrahman K, Fnais MS, Mickus K (2022) Understanding the structural framework controlling the sedimentary basins from the integration of gravity and magnetic data: a case study from the east of the Qattara Depression area, Egypt. *J King Saud Univ-Sci* 34(2):101808
- Salako KA (2014) Depth to basement determination using Source Parameter Imaging (SPI) of aeromagnetic data: an application to upper Benue Trough and Borno Basin, Northeast, Nigeria. *Acad Res Int* 5(3):74
- Salako KA, Udensi EE (2015) Two dimensional modeling of subsurface structure over upper Benue trough and Bornu basin in North eastern Nigeria. *Nigerian J Technol Res* 10(1):94–104
- Selim EI, Aboud E (2012) Determination of sedimentary cover and structural trends in the Central Sinai area using gravity and magnetic data analysis. *J Asian Earth Sci* 43(2012):193–206
- Smith RS, Thurston JB, Dai T, Macleod IN (1998) The improved source parameter imaging method. *Geophys Prospect* 46:141–151
- Talwani M, Walter K (2003) Exploration geophysics. *Encyclopedia of Physical Science and Technology* (Third Edition), pp 709 – 726
- Thurston JB, Smith RS (1997) Automatic conversion of magnetic data to depth dip, and susceptibility contrast using the SPI™ method. *Geophysics* 62:807–813
- Thurston JB, Smith RS, Guillon JC (2002) A multimodel method for depth estimation from magnetic data. *Geophysics* 67(2):555–561
- Thurston JB, Smith RS, Guillon JC (1999) Model-independent depth estimation with the SPI™ method. In: SEG technical program expanded abstracts, society of exploration geophysicists. pp 403–406
- Wang J, Yao C, Li Z, Zheng Y, Shen X, Zeren Z, Liu W (2020) 3D inversion of the Sichuan Basin magnetic anomaly in South China and its geological significance. *Earth, Planets and Space* 72(1):1–10
- Woakes M, Rahaman MA, Ajibade AC (1987) Some metallogenetic features of the Nigerian basement. *J Afr Earth Sc* 6(5):655–664
- Wright JB (1985) *Geology and mineral deposits of West Africa*. Allen and Unwin, London, p 189
- Zaborski PM, Ugodulunwa F, Idornigie A, Nnabo P, Ibe K (1998) Stratigraphy and structure of the Cretaceous Gongola basin, north-east Nigeria. *Bull Centres Rech Explor-Prod Elf-Aquitaine* 21(for 1997):153–185
- Zanguina M, Bruneton A, Gonnard R (1998) An introduction to the petroleum potential of Niger. *J Pet Geol* 21(1):83–103

Springer Nature or its licensor holds exclusive rights to this article under a publishing agreement with the author(s) or other rightsholder(s); author self-archiving of the accepted manuscript version of this article is solely governed by the terms of such publishing agreement and applicable law.